GANP Regulates the Choice of DNA Repair Pathway by DNA-PKcs Interaction in AID-Dependent *IgV* Region Diversification

Mohammed Mansour Abbas Eid,[1] Kazuhiko Maeda,[1] Sarah Ameen Almofty, Shailendra Kumar Singh, Mayuko Shimoda, and Nobuo Sakaguchi

RNA export factor germinal center–associated nuclear protein (GANP) interacts with activation-induced cytidine deaminase (AID) and shepherds it from the cytoplasm to the nucleus and toward the *IgV* region loci in B cells. In this study, we demonstrate a role for GANP in the repair of AID-initiated DNA damage in chicken DT40 B cells to generate *IgV* region diversity by gene conversion and somatic hypermutation. GANP plays a positive role in *IgV* region diversification of DT40 B cells in a nonhomologous end joining–proficient state. DNA-PKcs physically interacts with GANP, and this interaction is dissociated by dsDNA breaks induced by a topoisomerase II inhibitor, etoposide, or AID overexpression. GANP affects the choice of DNA repair mechanism in B cells toward homologous recombination rather than nonhomologous end joining repair. Thus, GANP presumably plays a critical role in protection of the rearranged *IgV* loci by favoring homologous recombination of the DNA breaks under accelerated AID recruitment. ***The Journal of Immunology*****, 2014, 192: 5529–5539.**

Antigen binding selectively induces the rapid proliferation and maturation of Ag-specific B cells. Ab maturation occurs with diversification of the rearranged *IgV* region gene segment by inducing activation-induced cytidine deaminase (AID) in the germinal centers of peripheral lymphoid organs (1–4). In mice and humans, *IgV* region diversification appears to occur with somatic hypermutation (SHM) accumulated nearby cytidines at WRC (W = A/T, R = A/G, and C) hotspot motifs (5, 6). The initial C deamination causes various DNA injuries, including DNA single-strand breaks and double-strand breaks (DSBs). Repair of these DNA injuries accompanies the high-frequency mutation during the process of mismatch repair (MMR) and base excision repair (BER) (7–13). In mammals, most DSBs occurring in various phases of the cell cycle are repaired by the nonhomologous end joining (NHEJ) repair mechanism, which is mediated by end-binding with Ku70 and Ku80 proteins catalyzed by DNA-PKcs (14–18). The DNA end joining is then catalyzed by DNA ligase IV, Artemis, and XRCC4. Such NHEJ repair potentially accompanies extreme sequence alterations because the DNA joining and extension do not read the template sequence and allow deletion or insertion of the nucleotide sequence during DNA ligation. NHEJ repair at the *IgV* region gene may predispose to the extensive alteration of the *V* region sequence, resulting in extinguishment of the Ag-binding capacity (19).

B cells, particularly in birds, diversify their *IgV* region repertoire through gene conversion (GCV). GCV involves alteration of the rearranged Ig L chain V region (IgV_L) sequence by copying a segment from one of the 25 upstream pseudo-*V* (ψV) donor gene sequences to the downstream IgV_L gene (20). The IgV_L GCV is well evidenced in the DT40 chicken B cell line (21–23). In the presence of AID and uracil nucleotide glycosidase (UNG), the IgV_L GCV is initiated with DNA injury and processed by a DNA repair mechanism similar to homologous recombination (HR) (23, 24). The HR DNA repair mechanism is employed against a large proportion of DNA damage responses associated with DNA replication at late S and G_2 phases of the cell cycle (11, 25). After invasion of the homologous chromosome aided by Rad51 recombinase, the HR repair response promotes the precise reading of the template DNA strand sequence using DNA polymerases, usually with error-free activity (DNA polymerase δ), but occasionally with error-prone activities such as in Ag-driven B cells to generate SHM (12, 26). In DT40 B cells, AID can induce both SHM and GCV at the IgV_L (24, 27). AID induces abundant IgV_L GCV in the presence of UNG, but predominantly induces SHM in UNG-deficient DT40 B cells (23). AID-initiated DNA injury is repaired through a DNA repair mechanism associated with GCV/HR and SHM in DT40 B cells, thus providing a suitable system to study the mechanisms of *IgV* region diversification after AID-induced DNA injuries.

Germinal center–associated nuclear protein (GANP) is upregulated in proliferating germinal center B cells (28–30). The central

Department of Immunology, Graduate School of Life Sciences, Kumamoto University, Kumamoto 860-8556, Japan

[1]M.M.A.E. and K.M. contributed equally to this work.

Received for publication January 8, 2014. Accepted for publication April 11, 2014.

This work was supported by Japan Society for the Promotion of Science (JSPS) Grants-in-Aid for Scientific Research 23390122, 24659224 (to N.S.), and 26460580 (to K.M.), the Ministry of Education, Culture, Sports, Science and Technology for Program of Japan Initiative for Global Research Network on Infectious Diseases (J-GRID) and the Advanced Education Program for Integrated Clinical, Basic, and Social Medicine (Graduate School of Life Sciences, Kumamoto University) (to M.M.A.E. and S.A.A.), JSPS Postdoctoral Fellowship for Foreign Researchers Grant-in-Aid P13407 (to S.K.S.), the Kumamoto University Program for Leading Graduate Schools "Health life science: Interdisciplinary and Glocal Oriented (HIGO)" Program (to M.S.), and grants from the Suzuken Memorial Foundation (to K.M.) and the Uehara Memorial Foundation (to N.S.).

Address correspondence and reprint requests to Prof. Nobuo Sakaguchi, Department of Immunology, Graduate School of Life Sciences, Kumamoto University, 1-1-1 Honjo, Chuo-ku, Kumamoto 860-8556, Japan. E-mail address: nobusaka@kumamoto-u.ac.jp

The online version of this article contains supplemental material.

Abbreviations used in this article: AID, activation-induced cytidine deaminase; AID^R, reconstituted AID; BER, base excision repair; ch-GANP, chicken germinal center–associated nuclear protein; Cpt, camptothecin; DSB, double-strand break; $DT40^{CL18}$, DT40 clone 18; Etp, etoposide; GANP, germinal center–associated nuclear protein; $GANP^{O/E}$, germinal center–associated nuclear protein overexpression; GCV, gene conversion; HR, homologous recombination; IgV_L, Ig L chain V region; IP, immunoprecipitation; MMR, mismatch repair; NHEJ, nonhomologous end joining; SHM, somatic hypermutation; sIgM, surface IgM; siRNA, small interfering RNA; TSA, trichostatin A; UNG, uracil nucleotide glycosidase; ψV, pseudo-V; WB, Western blot.

region of GANP is homologous to the *Saccharomyces cerevisiae* SAC3 protein, a component of the SAC3/THO complex involved in RNA export following transcription in yeast, and therefore GANP is proposed as a component of the mammalian transcription/export-2 complex (31, 32). Recently, we demonstrated that GANP interacts with cytoplasmic AID and assists its nuclear localization to augment its transport to the transcribed *IgV* region segment in B cells (33). In this process, the histone acetyltransferase region of GANP is involved in the selective recruitment of GANP toward the terminal region of the rearranged *IgV* region exons and the site-selective acetylation of the linker histone H1 (34). Thus, AID is targeted to the selective DNA region of the rearranged *IgV* loci with the assistance of GANP. AID converts C to U, creating a mismatch that can be processed by DNA-modifying enzymes such as UNG and APE1, leading to DNA breaks at the transcribed *IgV* region loci. AID interacts with the ribonucleoprotein complex, including RNA polymerase II, stall factor Spt5, and DNA-PKcs. DNA regions with DSBs initiated by intensive targeting of AID must be repaired during the interphase before the mitotic phase of the cell cycle to rescue and generate *IgV* region diversity in daughter Ag-reactive B cells. Our proteomics analysis revealed that GANP is associated with DNA-PKcs prominently among the DNA repair molecules (34). Given that GANP interacts with DNA-PKcs, it might be the initial member of the DNA repair pathway interacting with the AID/GANP complex in situ at the *IgV* region loci in germinal center B cells.

In this study, we demonstrate that GANP probably participates in the regulation of post-AID DNA repair during transcription-coupled *IgV* region diversification in B cells.

Materials and Methods

Plasmid construction

For GFP or GANP overexpression ($GANP^{O/E}$) transfectants, a GFP or GFP-GANP gene was introduced into pCXN2 (chicken β-actin promoter) vector containing a neomycin-resistant cassette (33). The AID expression vector (pFB-AID-IRES-GFP) was a gift from Dr. Tasuku Honjo (Kyoto University, Kyoto, Japan).

Antibodies

The following Abs were purchased: histone H4 (L64C1; Cell Signaling Technology), acetyl histone H4 (3HH4-4C10; Millipore), AID (L7E7 and 30F12; Cell Signaling Technology), β-actin (AC-15; Sigma-Aldrich), GANP (A303; Bethyl Laboratories), DNA-PKcs (sc-5282; Santa Cruz Biotechnology), phospho–DNA-PKcs (Thr^{2609}; 10B1; (BioLegend), Ku70 (sc-9033; Santa Cruz Biotechnology), mouse IgG (sc-2025; Santa Cruz Biotechnology), and biotinylated mouse anti-chicken IgM (M1) (SouthernBiotech).

DT40 cell lines and transfection

DT40 CL18 ($DT40^{CL18}$) (20), $AID^{-/-}\psi V^{-}$ (27), $AID^{-/-}UNG^{-/-}$ (23), and $Rad54^{-/-}$ (35), $Ku70^{-/-}$ (36) cells were cultured in IMDM supplemented with 0.1 mM 2-ME, 10% FBS, and 1% chicken serum (Tissue Culture Biologicals) at 39°C in a 5% CO_2 incubator and maintained by plating densities of $<3 \times 10^6$ cells/ml. To enhance the IgV_L GCV rate, 1.25 ng/ml trichostatin A (TSA; Wako, Osaka, Japan) was added to the culture medium. Transfections were performed by electroporating 1×10^7 cells with 30 μg linearized plasmid DNA at 550 V and 25 μF in PBS. After 24 h, the cells were resuspended in culture medium containing appropriate concentrations of the selection drugs: puromycin for the targeting vector, or G418 (Nacalai Tesque) for the other expression constructs. To establish $AID^{-/-}UNG^{-/-}GANP^{O/E}$ and reconstituted AID (AID^{R})$UNG^{-/-}GANP^{O/E}$ clones, the cells were sorted for expression of the GFP signal.

IgV_L *GCV assay*

The surface IgM (sIgM) was stained with a biotinylated mouse anti-chicken IgM (M1) Ab and secondary allophycocyanin-conjugated streptavidin (BD Biosciences). Dead cells were excluded by staining with 7-aminoactinomycin D (BD Biosciences). Single cells were plated from the $GFP^{+}IgM^{-}$ population into individual wells of 96-well plates using a JSAN cell sorter (Bay Bioscience), and the individual cells were expanded and examined for the rate of sIgM gain or loss using a flow cytometer (FACSCalibur, BD Biosciences). All data were analyzed using FlowJo software (Tree Star).

Sequencing of IgV_L

The $sIgM^{+}$ cells sorted with the JSAN were lysed with K buffer (PCR buffer containing 100 μg/ml proteinase K and 0.5% [v/w] Tween 20) for 2 h at 55°C. Aliquots were used as a template to amplify the rearranged allele of IgV_L with the primer set of IGL503 and IGL2903 (37) by PrimeSTAR HS polymerase (TaKaRa Bio). The PCR products were purified and ligated into the pCR4 Zero Blunt TOPO sequencing vector (Invitrogen). Plasmid DNA was purified using a DirectPrep 96 MiniPrep kit (Qiagen). Sequencing reactions were performed with a BigDye Terminator v1.1 kit (Applied Biosystems) and applied to an ABI 3130 sequencer (Applied Biosystems). Mutations and potential GCV tracts in the IgV_L sequence were determined by comparison with the known 25 ψV_L sequences, as reported previously (20).

Construction of chicken GANP targeting vector

The genomic structure of the *Gallus gallus mcm3ap* gene was surveyed using the database of the National Center for Biotechnology Information and partly confirmed by subcloning DNA fragments from DT40 cells by PCR. The targeting vector was constructed by replacing a 4.6-kb fragment encoding the chicken *GANP* (*ch-GANP*) open reading frame (from exon 6 to exon 10) with a floxed puromycin-resistance gene cassette (38) between the left arm (3.2 kb) and the right arm (2 kb). After the linearized targeting vector was transfected by electroporation, 34 drug-resistant clones were obtained after 10 d. PCR screening was carried out for the drug-resistant clones using the primer set of Ex5S (5′-GGCTGCAGTTTGAAGTCGATCTGTTCGA-3′) and Ex11AS (5′-CAGAGCGGTTCAGCTCCACATAAGTA-3′) to detect the targeting vector region, and the primer set of 5′-untranslated region 2 (5′-GGATCAGCACGCTCATGGCG-3′) and Puro (5′-CAGCGCCCGACCGAAAGGAGCGCACGACC-3′) to detect the targeted integration at the GANP allele. Six *ch-GANP* gene–haplodeficient DT40 clones ($GANP^{+/-}$) were established (targeting ratio, 17.6%; 6 clones from 34 clones).

RT-PCR, Northern blot, and Western blot

For RT-PCR analysis, total RNA samples were purified with an RNeasy Mini Kit (Qiagen) and reverse transcribed with SuperScript III reverse transcriptase (Invitrogen) according to the manufacturers' protocols. PCR was performed with following primer sets: human GANP, Ex5P (5′-GGCTGCAGTTTGAAGTCGATCTGTTCGA-3′) and Ex13P (5′-GGCTGCAGTCACGTAATCTGCTCCTGCTCT-3′), and β-actin, ACTIN1 (5′-CCC-CAAGCTTACTCCCACAGCCAGCCATGG-3′) and ACTIN2 (5′-GGCTCTAGATAGTCCGTCAGGTCACGGCCA-3′), respectively. For Northern blot analysis, the PCR-amplified cDNA fragments of *human-GANP* exon 1 (400 bp) and of ch-GANP3′-untranslated sequence (300 bp) were used as specific probes. Total RNA was extracted using TRIzol reagent (Invitrogen), electrophoresed, transferred onto nylon membrane, and then hybridized with the indicated radiolabeled probe as described elsewhere. For Western blot (WB) analysis, we prepared Abs against the ch-GANP protein by immunizing rabbits with various regions of the ch-GANP protein, which were produced in bacteria as recombinant fusion proteins with GST after subcloning the corresponding PCR-amplified cDNA fragments into the pET-41 vector (Novagen). As control blot, we used anti–β-actin Ab.

Chromatin immunoprecipitation–quantitative PCR

$GANP^{+/+}$ and $GANP^{+/-}$ were treated with 1.25, 2.5, and 5 nM of TSA (Wako) for 2 wk in RPMI 1640 culture medium containing 0.1 mM 2-ME, 10% FBS, and 1% chicken serum. Samples were prepared with anti-H4 and anti-acetyl H4 Abs (Cell Signaling Technology), as previously described (33, 34), and examined using Mesa Blue qPCR MasterMix Plus (Eurogentec) on the Applied Biosystems ViiA 7 with reported primers (37).

Quantitative real-time PCR analysis

RNA was prepared with a Cells-to-cDNA II kit (Ambion) and was reverse transcribed using a SuperScript III first-strand synthesis system (Invitrogen), and quantitative real-time PCR was performed using Mesa Blue qPCR MasterMix Plus (Eurogentec) on the Applied Biosystems 7500. Gene-specific primer sets were as follows: chicken AID, sense (5′-TATGTTGTGAAGCGCCGTGA-3′) and antisense (5′-ACCATGTGATGCGGTAGCAG-3′), and chicken HPRT1, sense (5′-TATTGTTGGAAC-

TGGAAGGACAATG-3′) and antisense (5′-ACTCACTGCTGTATATATTCATCAG-3′).

DNA repair assay

A modified pSVlacZ1351+727neo reporter was used for the NHEJ assay. Two HpaI sites of the β-galactosidase (*lacZ*) gene were mutated individually. Addition of two nucleotides converted the HpaI site to the XhoI site of the *lacZ* gene, which induced a frameshift and nonfunctional *lacZ* gene. The vector of recombination substrate was constructed by tandem alignment of two differently mutated *lacZ′* (at the second HpaI site) and *lacZ′′* (at the first HpaI site) genes. Flow cytometric measurements of β-galactosidase activity were carried out using the FluoReporter *lacZ* flow cytometry kit (Molecular Probes). For assessment of HR repair, the recombination reporter system, pDR-GFP, which contains a plasmid with two nonfunctional GFP genes and a recombinant plasmid encoding the restriction enzyme I-SceI, was used (39). The *5′ GFP* gene (*SceGFP*), mutated by insertion of an 18-mer restriction endonuclease site of I-SceI, produces a DSB once I-SceI is expressed (40). The truncated *3′ GFP* gene (*iGFP*) serves as a donor to correct the broken *SceGFP* gene, and the short tract GCV usually restores an intact *GFP* gene (41). Each clone was transiently transfected with vector for expression of I-SceI enzyme and GANP or empty expression vector.

Colony survival assay

Cells (500–1000 cells/well in a 96-well plate) were cultured in medium with varying concentrations of camptothecin (Cpt; Calbiochem) or etoposide (Etp; Calbiochem). After exposure to the drugs for 48 h, cells were stained with MTT dye (tetrazolium-based colorimetric assay; Roche) and measured at 595 nm according to the manufacturer's method. Cell survival rates were calculated as the percentage of surviving fraction after exposure to drugs relative to the control.

Cell cycle analysis

DT40 cells were harvested and washed once with PBS, then subcultured in six-well plates at concentration of 0.5×10^6 cells/ml in RPMI 1640 culture medium containing 0.1 mM 2-ME, 10% FBS, and 1% chicken serum for 24 h. Cells were then harvested, washed once with PBS, and stained with propidium iodide for 1 h. Data were collected using a FACSCalibur (Becton Dickinson). Data were analyzed with the FlowJo software (Tree Star).

Drug treatment in Ramos B cells

Ramos B cells were incubated in RPMI 1640 culture medium containing 0.1 mM 2-ME and 10% FBS with 50 μM Etp for 2 h, and then the medium was replaced with fresh culture medium and incubated for additional indicated periods. For kinase inhibition studies, cells were pretreated with 10 μM NU7026 (DNA-PKcs inhibitor; Sigma-Aldrich) for 1 h, and then incubated with 50 μM Etp for another 2 h in the presence of the inhibitor. After Etp treatment, cells were incubated in fresh medium with the inhibitor until cells were harvested.

Nuclease treatment

Cell extracts from Ramos nuclei were preincubated with either 250 μg/ml RNase A (Nippon Gene) or 50 U Turbo DNase I (Ambion) for 10 min before immunoprecipitation (IP).

Small interfering RNA treatment

Downregulation of AID with small interfering RNA (siRNA) in Ramos cells was carried out as described previously (42). Ramos cells (8×10^6 cells) were transfected with 2 μM siRNA using the Amaxa Nucleofector kit V (program O-06) according to the manufacturer's protocol. The duplex siRNA against human AID (AICDA; 5′-UUCAAAAAUGUCCGCUGGGCTT-3′) and negative control SIC were obtained from Sigma-Aldrich.

Statistical analysis

The statistical significance of differences among the groups was analyzed by an unpaired two-tailed Student *t* test. A p value <0.05 was considered statistically significant.

Results

GANP augments IgV_L *GCV in DT40 B cells*

We attempted to confirm the effect of GANP in an assay at the single cell level to measure *IgV* region diversification using chicken DT40 B cells. We examined $GANP^{O/E}$ by WB analysis of both endogenous chicken GANP and exogenous GANP following human GANP transfection of DT40 clone 18 ($DT40^{CL18}$) cells. $DT40^{CL18}GANP^{O/E}$ showed a 2- to 3-fold increase in GANP protein (Supplemental Fig. 1). $DT40^{CL18}$ carries the rearranged IgV_L with a frameshift mutation at nucleotide position 129 (by the G insertion) and therefore does not express sIgM. This frameshift is corrected by GCV, thus regaining sIgM expression (sIgM gain assay), which can be used to measure the frequency of GCV (Fig. 1A) (22, 24). The $DT40^{CL18}GANP^{O/E}$ clone significantly augmented the sIgM gain compared with the GFP-expressing $DT40^{CL18}$ ($DT40^{CL18}$GFP) clones (Fig. 1B). In comparison with the parental IgV_L sequence of $DT40^{CL18}$, the genomic sequence of the IgV_L showed GCV tracts from *ψV* donor segments in all the $sIgM^+$ cells (Fig. 1C). A higher rate of nonsense GCV tracts was found in $sIgM^-DT40^{CL18}GANP^{O/E}$ cells that failed to correct the IgV_L sequence to an in-frame position compared with control $DT40^{CL18}$GFP cells (Fig. 1D, after sequencing).

Next, we analyzed the usage of *ψV* genes as donor sequences, because a previous study demonstrated the preferential usage of *ψV8*, which showed the highest similarity to the rearranged IgV_L sequence (43). $DT40^{CL18}GANP^{O/E}$ cells used more diverse donor *ψV* genes with decreased usage of the preferential donor *ψV8* gene (52%), compared with the donor usage profile of $DT40^{CL18}$GFP (*ψV8* gene, 68%) (Fig. 1C, 1E). Additionally, the median tract length was also increased to 99 bp in $DT40^{CL18}GANP^{O/E}$ cells from 67 bp in $DT40^{CL18}$GFP cells, representing a significant stabilization of GCV with a donor tract of longer length (Fig. 1F). These results indicate that GANP plays a role in *IgV* region diversification by regulating the GCV/HR mechanism.

GANP is required for IgV_L *GCV in DT40 B cells*

We attempted to disrupt the *ch-GANP* gene by deleting the sequence encoded by the 6th to 10th exons in DT40 B cells (Supplemental Fig. 2A). Heterozygous GANP-deleted clones in $DT40^{CL18}$ ($GANP^{+/-}$) were selected using a puromycin-resistant gene, and the targeted regions were confirmed (Supplemental Fig. 2B). The mRNA and protein expression levels of ch-GANP in $GANP^{+/-}$ cells were estimated to be nearly half of parental $DT40^{CL18}$ ($GANP^{+/+}$) cells (Supplemental Fig. 2C, 2D). A subsequent attempt to delete another allele did not provide *GANP*-homodeficient clones even after repeated experiments. This observation was reminiscent of the embryonic lethality of *GANP*-deficient mice (30), indicating that GANP expression is essential for the maintenance of cells in certain stages of differentiation. Thus, ch-GANP may play an essential role in cellular maintenance for DT40 B cells that are proliferating and undergoing *IgV* region diversification.

We compared the fluctuation of sIgM gain in the $sIgM^-$ population from $GANP^{+/+}$ and $GANP^{+/-}$ cells during culture. The sIgM gain was significantly decreased during the culture of $GANP^{+/-}$ cells compared with $GANP^{+/+}$ cells (Fig. 2A). TSA is a histone deacetylase inhibitor, which increases IgV_L GCV (Fig. 2A), probably by activating the transcription rate through histone acetylation (37). TSA augments GCV significantly in $GANP^{+/+}$ DT40 cells, serving as a positive control and validating GCV data in our assay system compared with other laboratories (37, 44–46). The change in the gene dosage for endogenous GANP ($GANP^{+/+}$ versus $GANP^{+/-}$ cells) affected IgV_L GCV induced by TSA. This implies that GANP has a unique function in modulating the generation of IgV_L GCV over the enhanced transcription induced by the histone deacetylase inhibitor.

We further examined the effect of GANP in selective acetylation of both rearranged and unrearranged IgV_L loci using chromatin immunoprecipitation–quantitative PCR after TSA treatment of

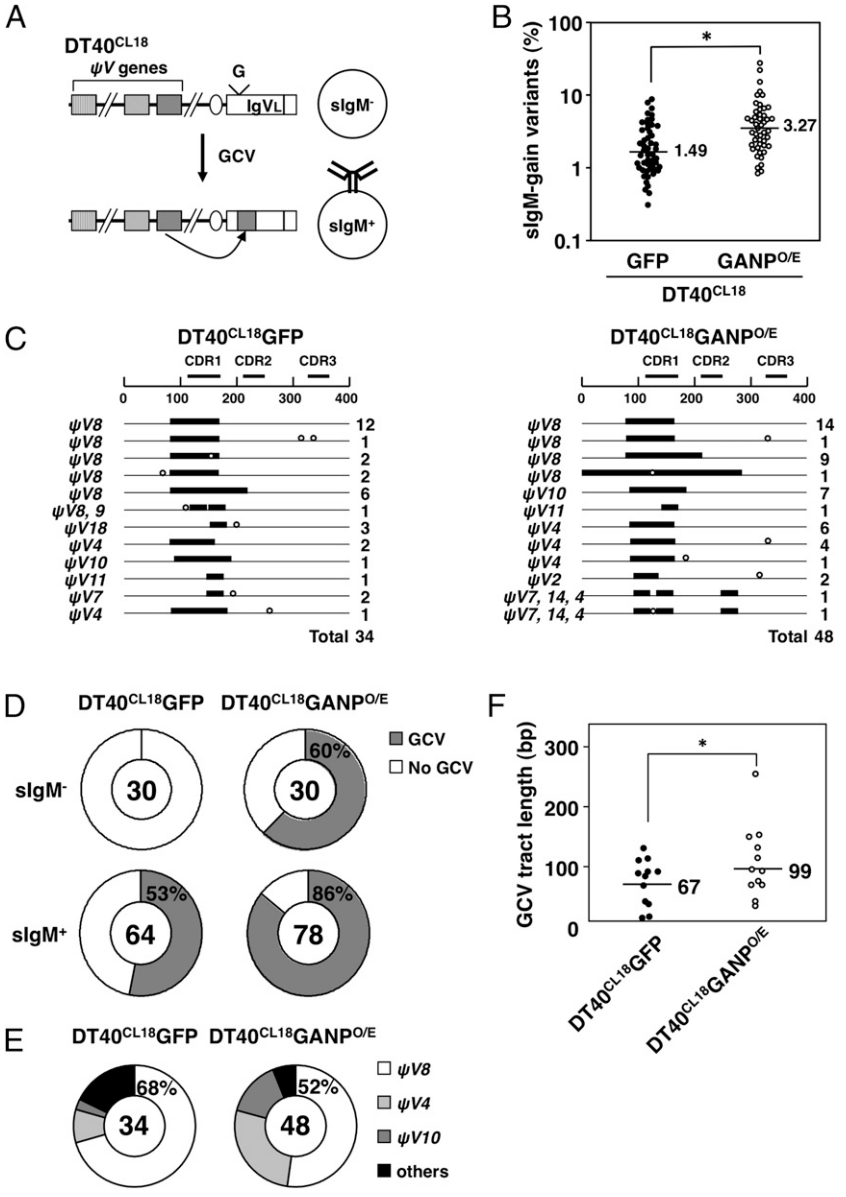

FIGURE 1. GANP regulates IgV_L GCV in DT40 B cells. (**A**) IgV_L GCV fluctuation assay. The original DT40^{CL18} carries a frameshift mutation in the rearranged IgV_L gene. The frameshift was eliminated by GCV, resulting in expression of sIgM. (**B**) Clonal analysis of sIgM gain. The rate of sIgM gain from sIgM$^-$ cells was clonally studied after culturing for 3 wk. Solid bars represent the median values. The difference between the rates of sIgM gain in DT40^{CL18}GFP (n = 52) and DT40^{CL18}GANP$^{O/E}$ (n = 51) clones was statistically significant (*$p < 0.02$). (**C**) IgV_L sequence analysis of cells showing sIgM gain between DT40^{CL18}GFP (*left*) and DT40^{CL18}GANP$^{O/E}$ (*right*) clones. Each horizontal line represents the IgV_L sequence region of parental CL18. The bold bars show the GCV tracts and the dots on the lines indicate point mutations. The donor ψV genes used are shown on the *left side*. The number of clones with each pattern is indicated on the *right side*. (**D**) The gray areas show the rate of IgV_L GCV in the pie graphs. The data were obtained from sIgM$^-$ (*upper*) and sIgM$^+$ (*lower*) populations. The number of sequences characterized is shown in the center of each graph. (**E**) Preferences for ψV gene usage as a donor sequence. The frequencies of the individual putative ψV genes among the total numbers of IgV_L sequences with GCV are shown. The total numbers of sequences analyzed are shown in the central circles. (**F**) Comparison of the GCV tract lengths. The tract length was analyzed by comparison with the known IgV_L sequences. *$p < 0.05$ by two-tailed unpaired t test.

GANP$^{+/+}$ and GANP$^{+/-}$ cells (37). GANP$^{+/-}$ cells failed to acetylate H4 to the same level as did control GANP$^{+/+}$ cells, markedly at 2 wk (Fig. 2B). Reduced H4 acetylation in GANP$^{+/-}$ cells suggests that GANP plays a role in augmenting TSA-induced chromatin modification selectively at the rearranged IgV_L. Sequence analysis showed that GCV was significantly reduced in GANP$^{+/-}$ cells (2.6%; 1 of 39 clones) compared with GANP$^{+/+}$ cells (34.9%; 15 of 43 clones) (Fig. 2C). These results confirmed that GANP is an integral molecule for regulation of the GCV/HR pathway to generate *IgV* region diversity.

GANP augments IgV_L *SHM in DT40 B cells*

AID induces IgV_L diversification in DT40 B cells with both GCV and SHM through a common intermediate (27). Under specific conditions lacking either the donor ψV segments or UNG, DT40 mutant cells selectively display AID-induced IgV_L SHM. In the assay for IgV_L SHM, we used another DT40 clone that expresses the productive IgV_L mRNA to express sIgM. IgV_L SHM is represented by the loss of sIgM from sIgM$^+$ cells and by sequencing of IgV_L in sIgM$^-$ cells (27). We measured the effect of GANP in generation of IgV_L SHM by introducing exogenous AID in DT40 B cells devoid of endogenous AID and ψV genes (AID$^{-/-}\psi V^-$). This type of cell is called AID^R in the original report (27) (Fig. 3A). AID$^R\psi V^-$ cells are DNA repair-proficient and devoid of any background GCV activity due to deletion of donor ψV segments, and therefore they represent an appropriate system to study the mechanism of AID-initiated SHM in further detail (23). The AID^R augmented the sIgM loss in AID$^{-/-}\psi V^-$ cells (Fig. 3B), confirming that AID is a primary requirement for generation of IgV_L SHM. GANP$^{O/E}$ significantly augmented sIgM loss by nearly 2-fold compared with mock-transfected AID$^R\psi V^-$ cells (Fig. 3B). The mutation analysis showed a pattern of mutations (transition versus transversion and G:C versus A:T) similar to that of AID$^R\psi V^-$ cells (Fig. 3C, Supplemental Fig. 3A), indicating that GANP does not affect the mutation pattern itself but rather augments the effect of AID.

To further address whether GANP is associated merely with the initial process of AID-dependent C deamination or also with the later DNA modifying error-prone mutational processes, we evaluated the SHM frequency on the basis of AID and UNG double-deficient DT40 cells (AID$^{-/-}$UNG$^{-/-}$) (Fig. 3D). The MSH-dependent MMR pathway is not functional in SHM in DT40 (47). AID-initiated lesions (C→U) create mutations after replication at G

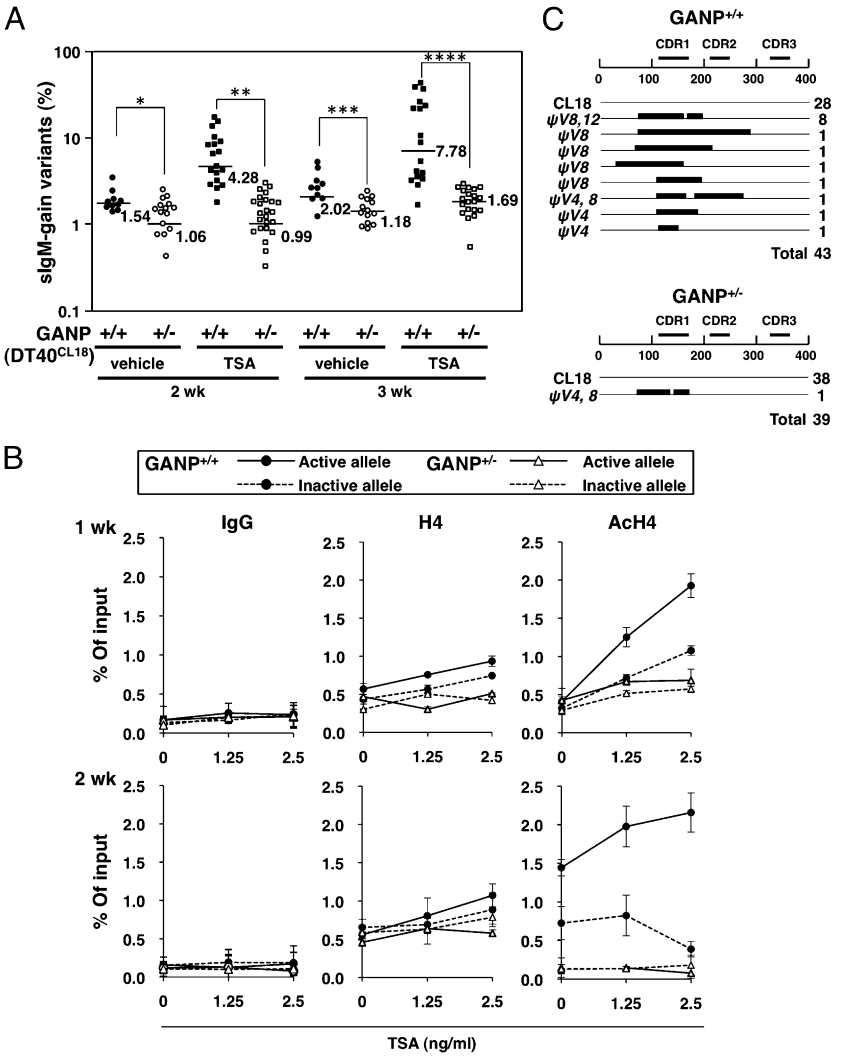

FIGURE 2. Effect of GANP haplodeficiency in IgV_L GCV in DT40 B cells. (**A**) The rate of sIgM gain was clonally studied after sorting of $sIgM^-$ cells and culturing for 2–3 wk with or without TSA. Each dot represents the percentage of $sIgM^+$ cells. Solid bars represent the median values. The difference between the rates of sIgM gain in $GANP^{+/+}$ (+/+; $n = 12$) and $GANP^{+/-}$ (−/−; $n = 18$) clones was statistically significant ($*p < 0.00085$, $**p < 0.005$, $***p < 0.002$, $****p < 0.002$). (**B**) Chromatin immunoprecipitation–quantitative PCR analysis of histone H4 acetylation at IgV_L after TSA treatment. The acetylation status of histone H4 both active (solid line) and inactive (dashed line) IgV_L loci were measured between $GANP^{+/+}$ (●) and $GANP^{+/-}$ (△) cells. IgG was used as the negative control. (**C**) Analysis of IgV_L sequence between the $GANP^{+/+}$ (*upper*) and $GANP^{+/-}$ (*lower*) clones after TSA treatment for 2 wk. Each horizontal line represents the IgV_L sequence region of CL18. The bold bars show the GCV tracts. The donor ψV genes used for the IgV_L GCV are shown on the *left side*. The number of clones with each pattern is indicated on the *right side*.

(G→A) and C (C→T) bases (22). Alternatively, the removal of U by UNG creates abasic sites followed by the nick and BER, creating transitions and transversions. $UNG^{-/-}$ cells predominantly create transition mutations at G:C. $GANP^{O/E}$ did not cause any change in sIgM loss in $AID^{-/-}UNG^{-/-}$ cells but augmented the sIgM loss ~2.2-fold (from 7.27 to 16.0%) in $AID^{R}UNG^{-/-}$ cells (Fig. 3E), confirming that GANP contributes to diversify IgV_L sequences in an AID-dependent manner. The viability of AID^{R} cells is similar to that of $AID^{-/-}$ cells even after $GANP^{O/E}$, indicating that AID expression is within harmless levels comparable to those of mutating B cells (Supplemental Fig. 3B). Notably, sequence analysis from sIgM loss variants showed that GANP augmented the SHM frequency (nearly 10-fold) with the C→T mutation (55.3%; 779 of 1409) at the predicted sense-strand DNA of the rearranged IgV_L gene (Fig. 3F, Supplemental Fig. 3C–E), which might agree with the observation that UNG favors IgV_L GCV but decreases SHM as reported (23). The mutation profile after $GANP^{O/E}$ showed predominance at G:C bases and mostly transitions similar to those of $UNG^{-/-}$ cells (23). The mutation profile also showed an increase in mutations at the putative CDRs (Supplemental Fig. 3F, 3G), which occurs selectively at the *V* region loci but not at the *C* region loci as GANP-mediated AID targeting (48). Supplemental Fig. 3H summarizes AID hotspot and coldspot preferences, suggesting that the specificity for hotspot targets is determined by AID itself. The transcription of chicken *AID* does not alter in $GANP^{+/+}$ and $GANP^{+/-}$ DT40 cells (Supplemental Fig. 3I). These results emphasize the conclusion that GANP augments the frequency of AID-initiated *IgV* region SHM in B cells, presumably through facilitating AID recruitment (33) and relaxing chromatin (34).

Effect of GANP on support of HR in the repair of DNA breaks

GANP interacts with DNA-PKcs in Ramos B cell nuclear extracts (34). This suggests a possible role of GANP in the regulation of the DNA repair mechanism required for generation of GCV. To investigate the function of GANP against DNA damage, two different DNA-damaging reagents, Etp and Cpt, were used. Etp is a topoisomerase II inhibitor that causes DNA DSBs that are mainly repaired by Artemis-independent NHEJ (49), even in the $S–G_2$ phase of the cell cycle (50). NHEJ-deficient DT40 cells are sensitive to Etp (51). $GANP^{O/E}$ rendered DT40 B cells more sensitive to Etp (Fig. 4A), suggesting a suppressive effect of GANP on NHEJ repair. In contrast, Cpt is a topoisomerase I inhibitor that causes DNA damages that are repaired exclusively by HR (52). DT40 cells lacking NHEJ repair function show resistance to Cpt-mediated cell death (15, 52), which is likely due to the release of the HR pathway from constitutive inhibition by the NHEJ pathway (14, 15, 19). $GANP^{O/E}$ rendered DT40 B cells resistant to Cpt-mediated cell death (Fig. 4B), confirming the enhanced functionality of GCV/HR by GANP expression. $GANP^{+/-}$ DT40 cells displayed the opposite results compared with those of $GANP^{O/E}$ cells in both Etp and Cpt treatments. Next, we examined

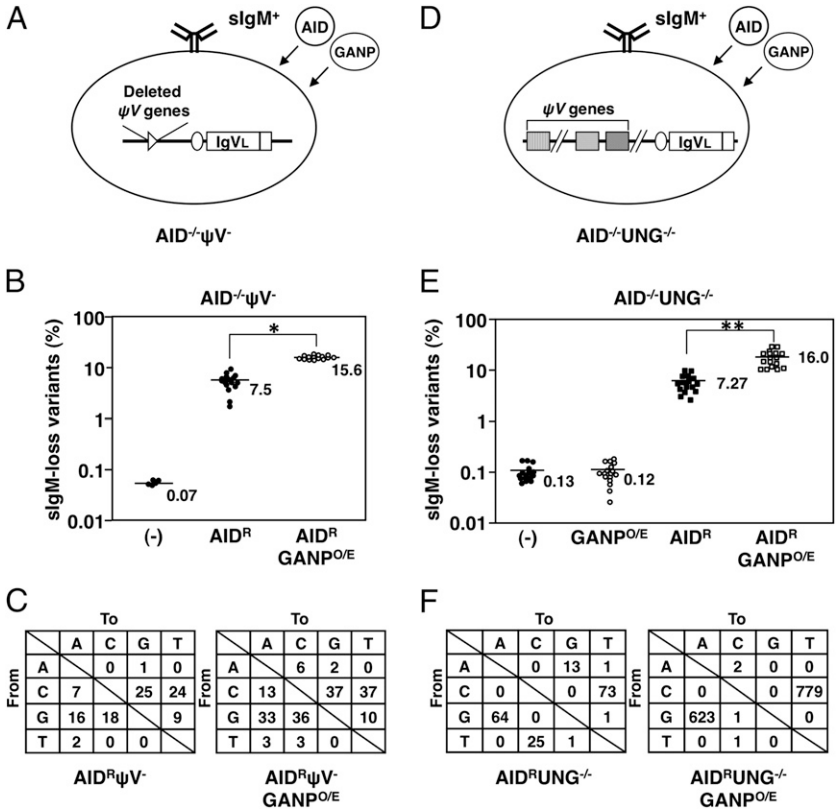

FIGURE 3. Regulation of IgV_L SHM by GANP via an AID- and UNG-dependent mechanism in DT40 B cells. (**A**) Scheme of the experiment using $AID^{-/-}\psi V^-$ cells. $AID^R\psi V^-$ cells were generated by reconstitution of the *AID* gene in $AID^{-/-}\psi V^-$ cells ($sIgM^+$ background). $AID^R\psi V^-$ cells induced mutations at IgV_L without GCV. $AID^R\psi V^-GANP^{O/E}$ cells were generated by introduction of *GANP* gene into $AID^R\psi V^-$ cells. (**B**) The rate of sIgM loss from $sIgM^+$ cells was clonally studied after culturing for 2 wk. Bars represent the median values. The difference between the rates of sIgM loss in $AID^R\psi V^-$ ($n = 16$) and $AID^R\psi V^-GANP^{O/E}$ ($n = 16$) clones was statistically significant ($^*p < 0.002$). (**C**) Patterns of nucleotide substitutions within IgV_L sequences from $AID^R\psi V^-$ (*left*) and $AID^R\psi V^-GANP^{O/E}$ (*right*) clones. (**D**) Scheme of the experiment using $AID^{-/-}UNG^{-/-}$ cells. $AID^{-/-}UNG^{-/-}GANP^{O/E}$ cells were generated by introduction of *GANP* cDNA into $AID^{-/-}UNG^{-/-}$ ($sIgM^+$ background). $AID^RUNG^{-/-}$ cells were generated by reconstitution of *AID* cDNA into $AID^{-/-}UNG^{-/-}$ cells. (**E**) The rate of sIgM loss variants was clonally studied after 1 wk. Each dot represents the percentage of $sIgM^-$ clones. Bars represent the median values. The difference between the rates of sIgM loss in $AID^RUNG^{-/-}$ ($n = 17$) and $AID^RUNG^{-/-}GANP^{O/E}$ ($n = 17$) clones was statistically significant ($^{**}p < 0.001$). (**F**) Patterns of nucleotide substitutions within IgV_L sequences from $AID^RUNG^{-/-}$ (*left*) and $AID^RUNG^{-/-}GANP^{O/E}$ (*right*) clones. The sIgM loss variants were sorted.

the effect of GANP more directly on DNA repair mechanisms with two kinds of reporter construct. First, we used stable transfectants with pSVlacZ reporter cassette for measuring the NHEJ frequency by lacZ color changes after spontaneous DNA breaks (Fig. 4C). The pSVlacZ vector contains two tandemly aligned and mutated *lacZ* genes, *lacZ′* and *lacZ′′*, with stop codons at the second HpaI and the first HpaI sites, respectively, precluding expression of productive lacZ. Deletion of the intervening segment led to reconstitution of the functional *lacZ* gene (Supplemental Fig. 4A). $GANP^{O/E}$ significantly reduced the frequency of $lacZ^+$ cells (Fig. 4D), probably as a consequence of suppressing NHEJ repair. The $lacZ^+$ frequency was markedly reduced in $Ku70^{-/-}$ cells (Supplemental Fig. 4B), confirming that DNA damage is predominantly repaired by NHEJ in this assay. Another reporter, pDR-GFP, can measure the frequency of GCV/HR DNA repair by the expression of GFP signal after induction of DSBs with I-SceI endonuclease (39) (Fig. 4E). In the present study, $GANP^{O/E}$ cells without GFP tag were used. $GANP^{O/E}$ increased the frequency of GFP^+ cells, indicating the positive effect of GANP on the DNA repair by GCV/HR (Fig. 4F). The altered expression of GANP either in $GANP^{+/-}$ or $GANP^{O/E}$ does not affect the cell cycle profile (Supplemental Fig. 4C). These data showed that GANP is likely to affect the DNA repair pathways against DSBs, primarily by negatively regulating NHEJ and conversely by promoting HR.

GANP regulates the choice of DNA repair mechanism between the NHEJ and HR pathways

DNA-PKcs is a core molecule in the NHEJ pathway but was recently identified to participate in regulation of the GCV/HR mechanism (53). In fact, DNA-PKcs has a strong suppressive effect on HR (54–56) and IgV_L GCV (19, 53) in DT40. We examined the effect of DNA-PKcs inhibitor NU7026 on spontaneous IgV_L GCV in $GANP^{+/+}$ and $GANP^{+/-}$ cells. NU7026 increased GCV rates by sIgM gain ~2-fold in $GANP^{+/+}$ cells (Fig. 5A). $GANP^{+/-}$ cells recovered the sIgM gain by GCV to levels comparable with wild-type $GANP^{+/+}$ cells in the presence of DNA-PKcs inhibitor. This supports that IgV_L GCV is mediated by reducing the influence of DNA-PKcs, presumably through interaction with GANP.

Previous reports demonstrated that the HR-deficient phenotype is rescued by abrogating NHEJ, reflecting that the repair process is dictated by a critical balance between NHEJ and HR (18) and not just by absolute presence or absence of the proteins that are functionally involved in both processes. To further analyze the regulatory role of GANP in the DNA repair mechanism, we examined whether GANP can restore the reduced GCV rate in HR-deficient DT40 cells. IgV_L GCV was examined in Rad54-deficient $DT40^{CL18}$ B cells ($Rad54^{-/-}$). $Rad54^{-/-}$ cells showed a decrease in IgV_L GCV due to their defective HR-mediated DNA repair (Fig. 5B) (35). Overexpression of GANP in $Rad54^{-/-}$ cells

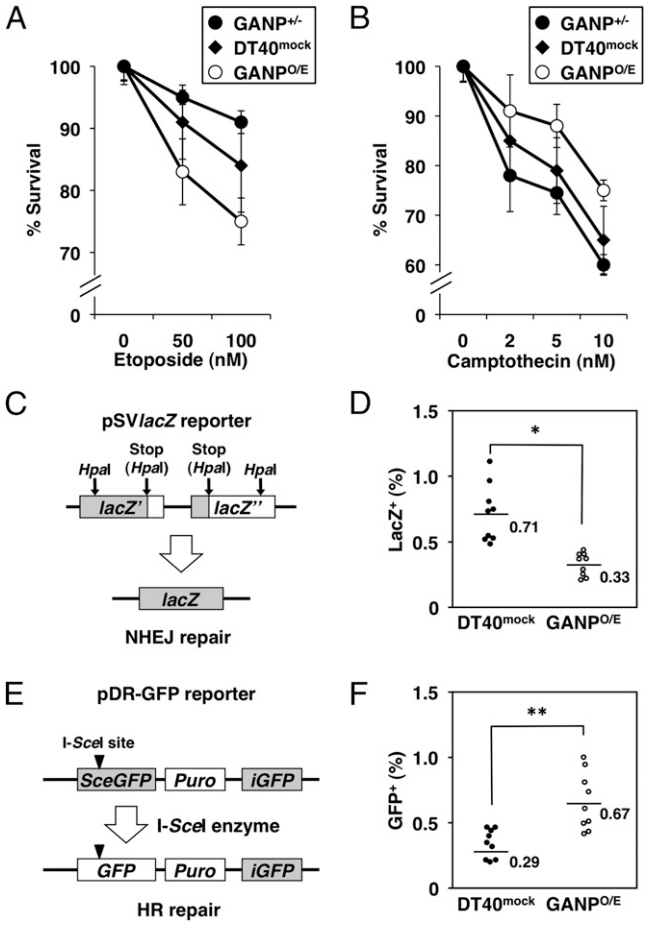

FIGURE 4. Effect of GANP on homology-directed DNA repair. (**A**) Sensitivity of GANP in DT40 clones to Etp. Cell survival rates from four different clones were calculated as the percentage of surviving fraction after exposure (48 h) to drugs relative to untreated cells. (**B**) Sensitivity of GANP in DT40 clones to Cpt. Cell survival rates from four different clones were calculated as the percentage of surviving fraction after exposure (48 h) to drugs relative to untreated cells. (**C**) Illustration of pSVlacZ reporter assay system. (**D**) Measurement of NHEJ repair using flow cytometric analysis of lacZ expression in mock-transfected (*left*) or GANP-transfected (*right*) clones. The difference between the rates of $lacZ^+$ cells in mock-transfected ($n = 9$) and GANP-transfected ($n = 9$) clones was statistically significant ($^*p < 0.05$). (**E**) Illustration of the pDR-GFP assay system. (**F**) Measurement of homology-directed DNA repair using flow cytometric analysis of GFP expression in mock-transfected (*left*) or GANP-transfected (*right*) clones. The difference between the rates of GFP^+ cells in mock-transfected ($n = 9$) and GANP-transfected ($n = 9$) clones was statistically significant ($^{**}p < 0.003$).

($Rad54^{-/-}GANP^{O/E}$) efficiently restored compromised GCV in $Rad54^{-/-}$ cells to levels almost comparable with those observed in $DT40^{CL18}GANP^{O/E}$ cells (Fig. 5B). The GCV tract of $Rad54^{-/-}GANP^{O/E}$ cells was similar to those of $DT40^{CL18}GANP^{O/E}$ and $Rad54^{-/-}GFP$ cells, as measured by sequence analysis (Figs. 1C, 5C). The ability of GANP to rescue the GCV/HR-deficient cells is compatible with the proposed role of GANP in abrogation of the NHEJ pathway. To confirm that GANP is targeting NHEJ, we transfected GANP in $Ku70^{-/-}$ cells lacking the NHEJ function to examine whether it still augments GCV/HR. $Ku70^{-/-}GFP$ cells showed the expected increase in GCV/HR compared with $DT40^{CL18}GFP$ cells owing to abolishment of NHEJ. Surprisingly, $Ku70^{-/-}GANP^{O/E}$ cells led to marked suppression of the GCV/HR rate compared with the control $Ku70^{-/-}GFP$ cells (Fig. 5D, 5E), supporting the notion that GANP plays a role in *IgV* region diversification through interacting with the functional NHEJ complex (54). Ku is thought to play a dominant negative effect in the absence of the DNA-PK–dependent NHEJ pathway that will limit the engagement of the other components (57, 58). The results might suggest that GANP influences the stability of the NHEJ complex. One possible explanation for the observed phenotype is that, in the absence of the physiological target of GANP in the functional NHEJ complex, GANP might stabilize their engagements upon NHEJ repair.

Alteration of GANP interaction with DNA-PKcs during DNA damage responses

GANP clearly interacted with DNA-PKcs even after treatment with DNase I or RNase A (Fig. 6A), indicating that their association is mediated through protein–protein interactions. DNA-PKcs is a core molecule in DNA break repair by NHEJ. We investigated whether GANP/DNA-PKcs association is DNA damage-dependent. First, the association of GANP and DNA-PKcs was examined after induction of DNA damage by AID. Remarkably, AID overexpression in Ramos B cells decreased DNA-PKcs coprecipitation with GANP (Fig. 6B); alternatively, AID knockdown does not alter their association. Etp-induced DNA damage decreased the GANP/DNA-PKcs association in a time-dependent manner in bidirectional IP/WB analyses (Fig. 6C). These results suggest that the interaction of GANP and DNA-PKcs is dissociated during the DNA damage response, particularly at 4 h after DNA breaks. AID-initiated DNA damage shows implicit dependence on DNA-PKcs for its repair (19, 59), and it is accompanied by DSBs that potentially augment the generation of *IgV* gene diversity in DT40 B cells (11, 27, 60). Etp-induced DNA breaks are dependent on NHEJ even in the $S–G_2$ phase of the cell cycle (50), and they require DNA-PKcs (61). The dissociation of DNA-PKcs from the GANP complex may affect the choice of DNA repair pathways at the selective site of DNA breaks targeted by GANP and its attendants.

DNA-PKcs is activated by phosphorylation at Thr^{2609} for NHEJ repair (54, 62). No association was detected between GANP and phospho–DNA-PKcs in IP/WB analysis (Fig. 6C). Once DNA-PKcs is phosphorylated at Thr^{2609}, it becomes fully activated and committed to NHEJ repair. This will cause the dissociation of phospho–DNA-PKcs from the GANP complex. Again, this finding consolidates the assumption that GANP binding to DNA-PKcs hinders its NHEJ repair capacity.

DNA-PKcs is thought to be a molecular sensor for DNA damage and the inducer of various DNA damage responses through phosphorylation of target molecules. A specific inhibitor of DNA-PKcs, NU7026, did not cause any change in the association of DNA-PKcs and GANP (Fig. 6D). Moreover, NU7026 could not inhibit the dissociation of DNA-PKcs from the GANP complex after treatment with Etp (Fig. 6E), indicating that their interaction is not dependent on the PI3K activity of DNA-PKcs itself. GANP and DNA-PKcs might be prerequisite components assembled for *IgV* region transcription-induced breaks involved in generation of *IgV* region diversity.

Discussion

The effect of GANP on *IgV* diversification was confirmed in a well-characterized system using chicken DT40 B cells in vitro. GANP highly augments the effect of AID on both GCV and SHM at the rearranged IgV_L locus. Moreover, GANP and DNA-PKcs association suggests an important role for GANP in regulating DNA repair pathways against AID-initiated DSBs. The results demonstrate that GANP favors the HR-mediated DNA repair pathway at the *IgV* region loci.

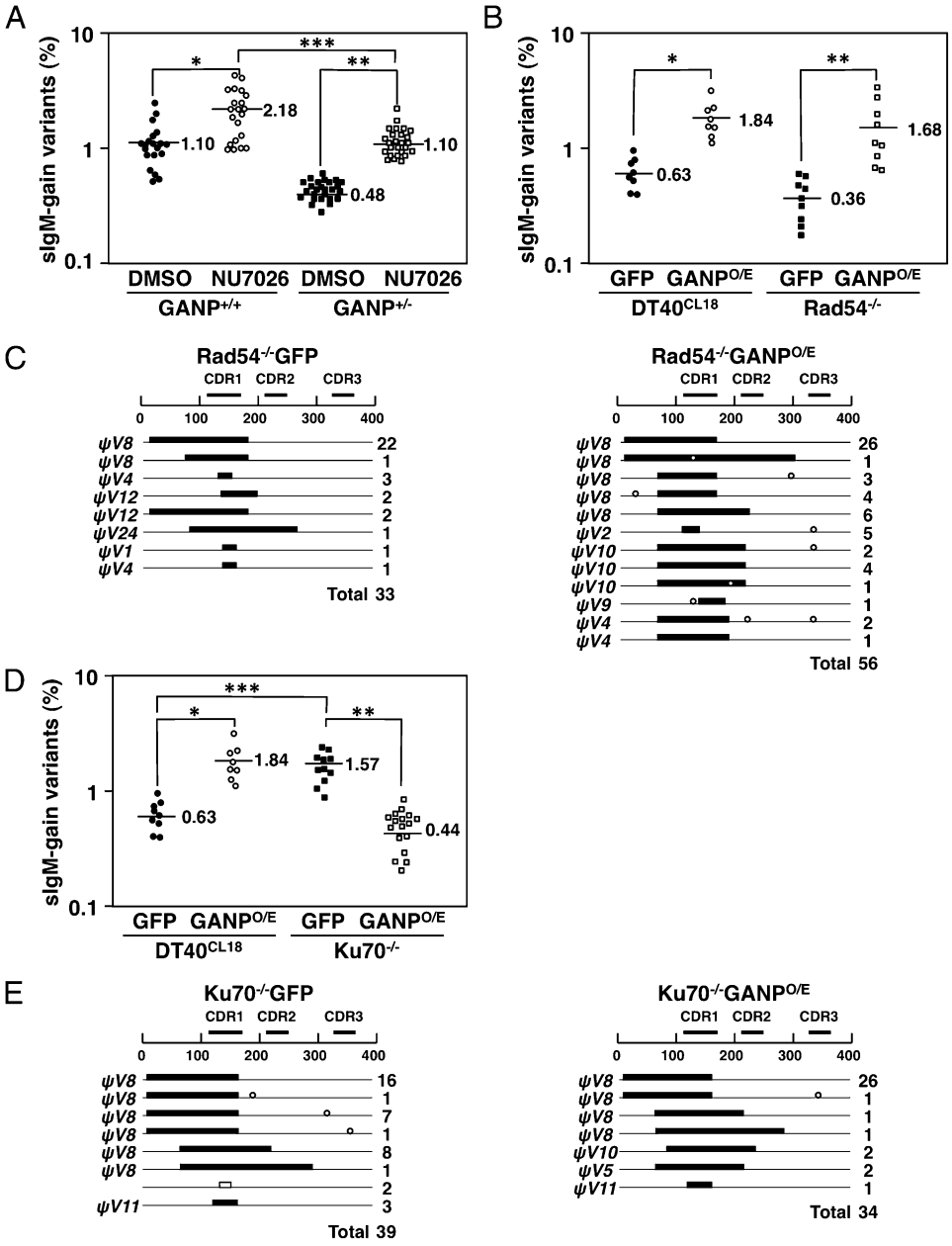

FIGURE 5. Effect of GANP on IgV_L GCV in mutant DT40 B cells with DNA repair deficiency. (**A**) The rate of sIgM gain was clonally studied after sorting of $sIgM^-$ cells and culturing for 2 wk. Each dot represents the percentage of $sIgM^+$ cells. Solid bars represent the median values. The difference between the rates of sIgM gain in DMSO-treated ($n = 28$) and in NU7026-treated ($n = 29$) $GANP^{+/+}$ clones was statistically significant ($^*p < 0.04$). The difference between the rates of sIgM gain in DMSO-treated ($n = 20$) and in NU7026-treated ($n = 20$) $GANP^{+/-}$ clones was statistically significant ($^{**}p < 0.01$). The difference between the rates of sIgM gain in NU7026 treatment of $GANP^{+/+}$ ($n = 29$) and $GANP^{+/-}$ ($n = 20$) clones was statistically significant ($^{***}p < 0.02$). (**B**) The rate of sIgM gain was clonally studied after sorting of $sIgM^-$ cells and culturing for 3 wk. Each dot represents the percentage of $sIgM^+$ cells. Solid bars represent the median values. The difference between the rates of sIgM gain in $DT40^{CL18}GFP$ ($n = 8$) and $DT40^{CL18}GANP^{O/E}$ ($n = 8$) clones was statistically significant ($^*p < 0.03$). The difference between the rates of sIgM gain in $Rad54^{-/-}GFP$ ($n = 9$) and $Rad54^{-/-}GANP^{O/E}$ ($n = 9$) clones was statistically significant ($^{**}p < 0.006$). (**C**) Summary of IgV_L sequences analysis of sIgM gain variants in $Rad54^{-/-}GFP$ (*left*) and $Rad54^{-/-}GANP^{O/E}$ clones (*right*). Each horizontal line represents the IgV_L sequence region of parental CL18. The bold bars show the GCV tracts, and dots on the lines indicate point mutations. The ψV genes used as donors are shown on the *left side*. The number of clones with each pattern is indicated on the *right side*. (**D**) The rate of sIgM gain was clonally studied after sorting $sIgM^-$ cells and culturing for 3 wk. Each dot represents the percentage of $sIgM^+$ cells. Solid bars represent the median values. The difference between the rates of sIgM gain in $DT40^{CL18}GFP$ ($n = 9$) and $DT40^{CL18}GANP^{O/E}$ ($n = 9$) clones was statistically significant ($^*p < 0.03$). The difference between the rates of sIgM gain in $Ku70^{-/-}GFP$ ($n = 11$) and $Ku70^{-/-}GANP^{O/E}$ ($n = 17$) clones was statistically significant ($^{**}p < 0.001$). The difference between the rates of sIgM gain in $DT40^{CL18}GFP$ ($n = 9$) and $Ku70^{-/-}GFP$ ($n = 11$) clones was statistically significant ($^{***}p < 0.02$). (**E**) Summary of IgV_L sequence analyses of sIgM gain variants in $Ku70^{-/-}GFP$ (*left*) and $Ku70^{-/-}GANP^{O/E}$ clones (*right*). Each horizontal line represents the IgV_L sequence region of parental CL18. The bold bars show the GCV tracts and dots on the lines indicate point mutations. The ψV genes used as donors are shown on the *left side*. The number of clones with each pattern is indicated on the *right side*.

AID-initiated DNA injuries can be repaired by various pathways (12, 63–66). AID attacks and creates DNA single-strand breaks, and DSBs result when these occur on the opposite strand within a localized region. This is further confirmed by the fact that AID attacks C on both strands simultaneously (67). AID-initiated DSBs are the intermediates in IgV_L SHM and GCV (12, 19, 26, 53), and

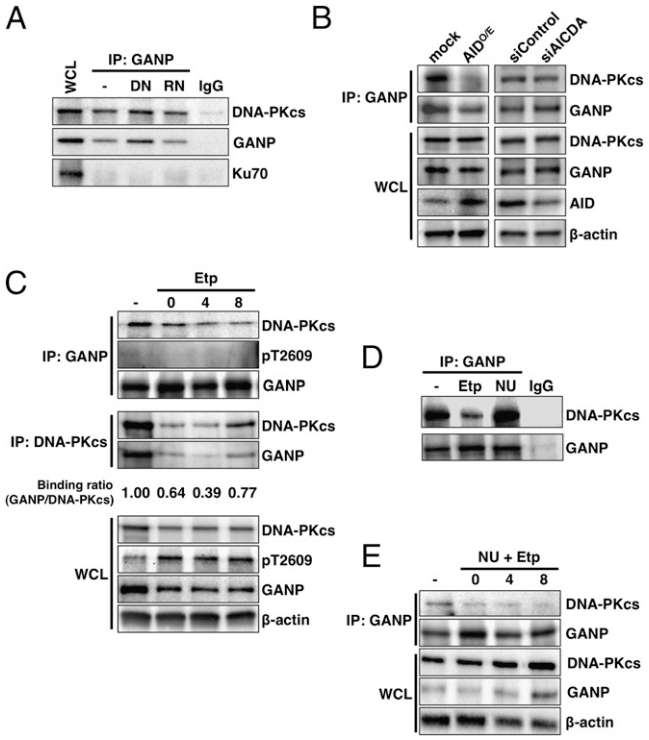

FIGURE 6. DNA-PKcs dissociates from the GANP complex following induction of DNA DSBs. (**A**) Ramos B cell nuclear extracts were either untreated (−), treated with DNase I (DN), or treated with RNase A (RN) before IP. IgG was used as a negative control. (**B**) AID overexprssion ($AID^{O/E}$) affects the interaction between GANP and DNA-PKcs. IP analysis of Ramos B cells after mock or AID transfection and small interfering (si)Control or siAICDA knockdown is shown. IP was performed with anti-GANP Ab and blotted with anti–DNA-PKcs and anti-GANP Abs. (**C**) DNA-PKcs dissociates from GANP after Etp treatment. Ramos B cells were incubated with 50 μM Etp for 2 h. After Etp treatment, cells were harvested at indicated time points (0, 4, and 8 h). Untreated whole-cell lysates (WCLs) (−) were used as a loading control. The relative GANP binding ratio with DNA-PKcs after Etp treatment was measured by densitometric analysis. (**D**) NU7026 does not affect the GANP/DNA-PKcs complex. Ramos B cells were either untreated (−) or Etp- (50 μM) or NU7026 (NU; 10 μM) treated before IP with anti-GANP Ab. IgG was used as a negative control for WB. (**E**) Effect of Etp and a DNA-PKcs inhibitor. Ramos B cells were either untreated (−) or treated with Etp and NU before IP with anti-GANP Ab. Untreated WCLs (−) were used as loading controls. Data are from one of three independent experiments with similar results.

HR and NHEJ are the two conserved main pathways evolved to deal with DNA breaks, from yeast to vertebrates. HR plays a dominant role in DSB repair in yeast, whereas NHEJ is the predominant repair mechanism in vertebrates, including birds. The high activity and predominance of NHEJ necessitates the evolution of regulatory mechanisms to choose between HR or NHEJ in vertebrate cells (15). Although DT40 cells are commonly used for their very high rate of gene targeting through HR, NHEJ remains a predominant repair mechanism in DT40 cells. NHEJ repair poses significant competition or hindrance for GCV/HR, both at the level of GCV and *IgV* region diversification (19, 21, 53), as well as at the level of general HR in DSB repair (52). From our data, abrogating NHEJ in $Ku70^{-/-}$, a core NHEJ molecule, greatly augments GCV/HR compared with $DT40^{CL18}$GFP (Fig. 5D). Thus, the critical regulation and the balance or choice between these pathways finally impacts GCV/HR outcome and determines the genetic integrity of cells in the presence of different DNA damaging stresses.

Many factors, including DNA-PKcs, can regulate the mechanistic overlap or competition between NHEJ and HR (16, 53–55, 68). DNA-PKcs suppresses both spontaneous and DSB-induced HR at the initial step of DNA repair (56). This was clearly demonstrated by its suppression of GCV in DT40 cells (19, 53). The promotion of GCV/HR by GANP (Fig. 1), together with its binding to DNA-PKcs (Fig. 6A) (34), supports a model in which the regulation of DNA-PKcs could promote GCV/HR through abrogating the competing NHEJ pathway (Fig. 7). GANP clearly suppresses NHEJ, as demonstrated using a LacZ construct (Fig. 4D), and promotes HR, as shown using a pDR-GFP construct (Fig. 4F). These results confirmed that GANP possesses a regulatory function in DNA repair in DT40 cells and mammalian cells. This is further solidified using two different DNA DSB inducers, Etp and Cpt. $GANP^{O/E}$ rescued Cpt-induced cell death but markedly reduced the survival of Etp-treated cells (Fig. 4A). Thus, GANP could participate in the choice of DNA repair pathways at the actively transcribed genes in situ to use the adequate DNA repair response. Reduction of GCV/HR in $GANP^{+/-}$ cells may be partly due to defective transcription (Fig. 2B); nevertheless, NU7026 DNA-PKcs kinase inhibitor could markedly recover the GCV/HR rate in $GANP^{+/-}$ cells (Fig. 5A), indicating that diminished GCV/HR in these cells is largely due to the enhanced NHEJ function rather than the defective transcription. These results signify that GANP supports GCV/HR through suppressing the NHEJ pathway.

The DT40 cell is unique in the genomic IgV_L region configuration with a single productive *V* segment and the ψV segments

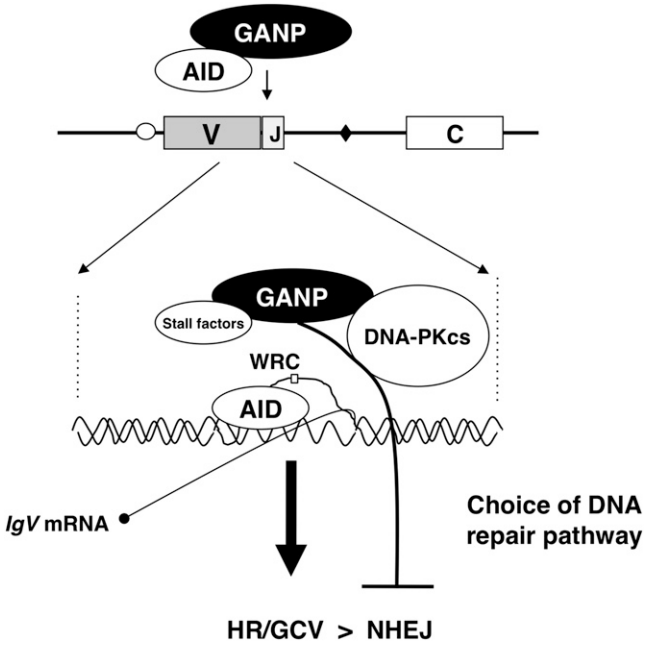

FIGURE 7. A model of GANP-mediated DNA repair. Ag-driven B cells undergo *IgV* region SHM in germinal centers or alternatively *IgV* region GCV and SHM in avian DT40 B cells, with increased expression of AID and GANP. The AID/GANP complex is shepherded into the nucleus and recruited to the nucleosome of the rearranged *IgV* region DNA (33, 34). The nucleosome is relaxed by the arrival of GANP together with AID. AID catalyses the deamination of C at the consensus WRC (W = A/T, R = A/G, and C) motif on the ssDNA formed in an R loop with the stall factors during active transcription, and presumably initiates DNA breaks with the intensive AID targeting. GANP, in turn, associates with DNA-PKcs and possibly inhibits its local mobilization to injured DNA sites or functionally disturbs NHEJ. This might play a role in the inhibition of NHEJ DNA repair locally at the rearranged *IgV* region to maintain its integrity.

located in close proximity, which predominantly leads to GCV rather than SHM. In mammals, four types of molecular mechanisms deal with AID-initiated injuries: BER, MMR, HR, and NHEJ. With the exception of NHEJ, SHM was shown to be mediated through BER, MMR, and unexpectedly also through HR (12, 26), suggesting that the generation of SHM might be generated on the balance of these DNA repair pathways and affected by the genomic gene configurations. GANP promotes *IgV* SHM in $AID^{R}\psi V^{-}$ and $AID^{R}UNG^{-/-}$ cells, supporting that GANP is not acting as a negative regulator of SHM. Similar to BER and MMR, the HR repair is an error-free repair pathway by default; however, in particular conditions, these pathways are chosen by B cells and subverted to be mutagenic rather than faithful. During generation of *IgV* SHM (69, 70), B cells might often sustain extensive genomic alterations such as translocations, deletions, and duplications. GANP is not only involved in selective AID targeting to the rearranged *IgV* loci (33, 34), but also in the process of post-AID–mediated DNA breaks through promoting HR via abrogating NHEJ (Figs. 4, 5). This will favor the maintenance of the *IgV* region structure and its functional integrity by preventing translocations, truncations, and deletions of the rearranged *Ig* genes that inevitably cause the extinguishment of Ab maturation (19).

The effect of inactive DNA-PKcs on *IgV* SHM has been characterized in a system using a special mouse carrying the rearranged IgM-IgD, κ gene transgenes for hen egg lysozyme on the SCID background (71), because DNA-PKcs-null or inactive mice could not generate B cells. The mutant mice did not exhibit apparent changes in the total SHM frequency of germinal center B cells after immunization but demonstrated a change in SHM pattern with increased G:C mutations and decreased C:T mutations. In another study using a similar mutant mouse model, B cells from SCID mice similarly showed skewing of the mutation pattern, affecting C residues on the sense strand (72). These studies imply that total absence of DNA-PKcs may not influence the frequency of *IgV* SHM; nevertheless, kinase deficiency and probably functionally disturbed DNA-PKcs impact the mutation pattern.

To generate Ag-specific and high-affinity B cell clones, regulation of the repair of post-AID–initiated DNA damage is inevitable. Our data suggest that GANP is associated with AID and reduces the level of functionality of NHEJ at the sites of AID-mediated DNA breaks in situations where HR is required to induce repair, such as replication and/or transcription block, SHM, and GCV. DNA-PKcs might initiate immediate DNA repair at the damaged DNA region through activation of the NHEJ pathway when the DNA damage is minimal. However, the binding of GANP with DNA-PKcs, or its interaction with the NHEJ-dependent pathway, directs the repair toward the HR pathway at the transcriptionally active *IgV* region loci (Fig. 7). This would ensure, according to the local context, the choice of the proper repair pathway required for preserving viability of B cells and functional integrity of *IgV* region loci.

In summary, GANP plays multifunctional roles in regulation of *IgV* region diversification, as follows: 1) change of chromatin conformation, 2) recruitment and selective targeting of AID to the rearranged *IgV* region loci, and 3) choice of DNA repair pathway against post-AID–initiated DNA breaks. The latter would be beneficial to induce *IgV* region diversification for affinity maturation of germinal center B cells.

Acknowledgments

We thank Shunichi Takeda, Eiichiro Sonoda, Minoru Takada, Hideki Koyama, and Jean-Marie Buerstedde for the DT40 mutants. We thank Maria Jasin for the site-specific DNA repair vector. We thank Yoshimi Fukushima and Kazufumi Eda for assistance.

Disclosures

The authors have no financial conflicts of interest.

References

1. Maul, R. W., and P. J. Gearhart. 2010. AID and somatic hypermutation. *Adv. Immunol.* 105: 159–191.
2. Odegard, V. H., and D. G. Schatz. 2006. Targeting of somatic hypermutation. *Nat. Rev. Immunol.* 6: 573–583.
3. Peled, J. U., F. L. Kuang, M. D. Iglesias-Ussel, S. Roa, S. L. Kalis, M. F. Goodman, and M. D. Scharff. 2008. The biochemistry of somatic hypermutation. *Annu. Rev. Immunol.* 26: 481–511.
4. Di Noia, J. M., and M. S. Neuberger. 2007. Molecular mechanisms of antibody somatic hypermutation. *Annu. Rev. Biochem.* 76: 1–22.
5. Pham, P., R. Bransteitter, J. Petruska, and M. F. Goodman. 2003. Processive AID-catalysed cytosine deamination on single-stranded DNA simulates somatic hypermutation. *Nature* 424: 103–107.
6. Bransteitter, R., P. Pham, M. D. Scharff, and M. F. Goodman. 2003. Activation-induced cytidine deaminase deaminates deoxycytidine on single-stranded DNA but requires the action of RNase. *Proc. Natl. Acad. Sci. USA* 100: 4102–4107.
7. Chahwan, R., W. Edelmann, M. D. Scharff, and S. Roa. 2011. Mismatch-mediated error prone repair at the immunoglobulin genes. *Biomed. Pharmacother.* 65: 529–536.
8. Sharbeen, G., C. W. Yee, A. L. Smith, and C. J. Jolly. 2012. Ectopic restriction of DNA repair reveals that UNG2 excises AID-induced uracils predominantly or exclusively during G_1 phase. *J. Exp. Med.* 209: 965–974.
9. Frieder, D., M. Larijani, C. Collins, M. Shulman, and A. Martin. 2009. The concerted action of Msh2 and UNG stimulates somatic hypermutation at A·T base pairs. *Mol. Cell. Biol.* 29: 5148–5157.
10. Liu, M., and D. G. Schatz. 2009. Balancing AID and DNA repair during somatic hypermutation. *Trends Immunol.* 30: 173–181.
11. Tang, E. S., and A. Martin. 2007. Immunoglobulin gene conversion: synthesizing antibody diversification and DNA repair. *DNA Repair (Amst.)* 6: 1557–1571.
12. Zan, H., X. Wu, A. Komori, W. K. Holloman, and P. Casali. 2003. AID-dependent generation of resected double-strand DNA breaks and recruitment of Rad52/Rad51 in somatic hypermutation. *Immunity* 18: 727–738.
13. Reynaud, C. A., F. Delbos, A. Faili, Q. Guéranger, S. Aoufouchi, and J. C. Weill. 2009. Competitive repair pathways in immunoglobulin gene hypermutation. *Philos. Trans. R. Soc. Lond. B Biol. Sci.* 364: 613–619.
14. Mansour, W. Y., S. Schumacher, R. Rosskopf, T. Rhein, F. Schmidt-Petersen, F. Gatzemeier, F. Haag, K. Borgmann, H. Willers, and J. Dahm-Daphi. 2008. Hierarchy of nonhomologous end-joining, single-strand annealing and gene conversion at site-directed DNA double-strand breaks. *Nucleic Acids Res.* 36: 4088–4098.
15. Sonoda, E., H. Hochegger, A. Saberi, Y. Taniguchi, and S. Takeda. 2006. Differential usage of non-homologous end-joining and homologous recombination in double strand break repair. *DNA Repair (Amst.)* 5: 1021–1029.
16. Neal, J. A., and K. Meek. 2011. Choosing the right path: does DNA-PK help make the decision? *Mutat. Res.* 711: 73–86.
17. Meek, K., S. Gupta, D. A. Ramsden, and S. P. Lees-Miller. 2004. The DNA-dependent protein kinase: the director at the end. *Immunol. Rev.* 200: 132–141.
18. Patel, A. G., J. N. Sarkaria, and S. H. Kaufmann. 2011. Nonhomologous end joining drives poly(ADP-ribose) polymerase (PARP) inhibitor lethality in homologous recombination-deficient cells. *Proc. Natl. Acad. Sci. USA* 108: 3406–3411.
19. Tang, E. S., and A. Martin. 2006. NHEJ-deficient DT40 cells have increased levels of immunoglobulin gene conversion: evidence for a double strand break intermediate. *Nucleic Acids Res.* 34: 6345–6351.
20. Buerstedde, J. M., C. A. Reynaud, E. H. Humphries, W. Olson, D. L. Ewert, and J. C. Weill. 1990. Light chain gene conversion continues at high rate in an ALV-induced cell line. *EMBO J.* 9: 921–927.
21. Paddock, M. N., A. T. Bauman, R. Higdon, E. Kolker, S. Takeda, and A. M. Scharenberg. 2011. Competition between PARP-1 and Ku70 control the decision between high-fidelity and mutagenic DNA repair. *DNA Repair (Amst.)* 10: 338–343.
22. Arakawa, H., and J. M. Buerstedde. 2009. Activation-induced cytidine deaminase-mediated hypermutation in the DT40 cell line. *Philos. Trans. R. Soc. Lond. B Biol. Sci.* 364: 639–644.
23. Saribasak, H., N. N. Saribasak, F. M. Ipek, J. W. Ellwart, H. Arakawa, and J. M. Buerstedde. 2006. Uracil DNA glycosylase disruption blocks Ig gene conversion and induces transition mutations. *J. Immunol.* 176: 365–371.
24. Arakawa, H., J. Hauschild, and J. M. Buerstedde. 2002. Requirement of the activation-induced deaminase (AID) gene for immunoglobulin gene conversion. *Science* 295: 1301–1306.
25. Chapman, J. R., M. R. Taylor, and S. J. Boulton. 2012. Playing the end game: DNA double-strand break repair pathway choice. *Mol. Cell* 47: 497–510.
26. Papavasiliou, F. N., and D. G. Schatz. 2000. Cell-cycle-regulated DNA double-stranded breaks in somatic hypermutation of immunoglobulin genes. *Nature* 408: 216–221.
27. Arakawa, H., H. Saribasak, and J. M. Buerstedde. 2004. Activation-induced cytidine deaminase initiates immunoglobulin gene conversion and hypermutation by a common intermediate. *PLoS Biol.* 2: E179.
28. Kuwahara, K., M. Yoshida, E. Kondo, A. Sakata, Y. Watanabe, E. Abe, Y. Kouno, S. Tomiyasu, S. Fujimura, T. Tokuhisa, et al. 2000. A novel nuclear phosphoprotein, GANP, is up-regulated in centrocytes of the germinal center and associated with MCM3, a protein essential for DNA replication. *Blood* 95: 2321–2328.

29. Fujimura, S., K. Kuwahara, T. Ezaki, K. Tomita, S. Hirose, and N. Sakaguchi. 2003. Spontaneous increase of plasma-like cells with high GANP expression in the extrafollicular region of lymphoid organs of autoimmune-prone mice. *J. Autoimmun.* 20: 291–301.
30. Sakaguchi, N., K. Maeda, and K. Kuwahara. 2011. Molecular mechanism of immunoglobulin V-region diversification regulated by transcription and RNA metabolism in antigen-driven B cells. *Scand. J. Immunol.* 73: 520–526.
31. Wickramasinghe, V. O., P. I. McMurtrie, A. D. Mills, Y. Takei, S. Penrhyn-Lowe, Y. Amagase, S. Main, J. Marr, M. Stewart, and R. A. Laskey. 2010. mRNA export from mammalian cell nuclei is dependent on GANP. *Curr. Biol.* 20: 25–31.
32. Jani, D., S. Lutz, E. Hurt, R. A. Laskey, M. Stewart, and V. O. Wickramasinghe. 2012. Functional and structural characterization of the mammalian TREX-2 complex that links transcription with nuclear messenger RNA export. *Nucleic Acids Res.* 40: 4562–4573.
33. Maeda, K., S. K. Singh, K. Eda, M. Kitabatake, P. Pham, M. F. Goodman, and N. Sakaguchi. 2010. GANP-mediated recruitment of activation-induced cytidine deaminase to cell nuclei and to immunoglobulin variable region DNA. *J. Biol. Chem.* 285: 23945–23953.
34. Singh, S. K., K. Maeda, M. M. Eid, S. A. Almofty, M. Ono, P. Pham, M. F. Goodman, and N. Sakaguchi. 2013. GANP regulates recruitment of AID to immunoglobulin variable regions by modulating transcription and nucleosome occupancy. *Nat. Commun.* 4: 1830.
35. Bezzubova, O., A. Silbergleit, Y. Yamaguchi-Iwai, S. Takeda, and J. M. Buerstedde. 1997. Reduced x-ray resistance and homologous recombination frequencies in a RAD54$^{-/-}$ mutant of the chicken DT40 cell line. *Cell* 89: 185–193.
36. Takata, M., M. S. Sasaki, E. Sonoda, C. Morrison, M. Hashimoto, H. Utsumi, Y. Yamaguchi-Iwai, A. Shinohara, and S. Takeda. 1998. Homologous recombination and non-homologous end-joining pathways of DNA double-strand break repair have overlapping roles in the maintenance of chromosomal integrity in vertebrate cells. *EMBO J.* 17: 5497–5508.
37. Seo, H., M. Masuoka, H. Murofushi, S. Takeda, T. Shibata, and K. Ohta. 2005. Rapid generation of specific antibodies by enhanced homologous recombination. *Nat. Biotechnol.* 23: 731–735.
38. Arakawa, H., D. Lodygin, and J. M. Buerstedde. 2001. Mutant loxP vectors for selectable marker recycle and conditional knock-outs. *BMC Biotechnol.* 1: 7.
39. Pierce, A. J., R. D. Johnson, L. H. Thompson, and M. Jasin. 1999. XRCC3 promotes homology-directed repair of DNA damage in mammalian cells. *Genes Dev.* 13: 2633–2638.
40. Richardson, C., M. E. Moynahan, and M. Jasin. 1998. Double-strand break repair by interchromosomal recombination: suppression of chromosomal translocations. *Genes Dev.* 12: 3831–3842.
41. Bechter, O. E., Y. Zou, J. W. Shay, and W. E. Wright. 2003. Homologous recombination in human telomerase-positive and ALT cells occurs with the same frequency. *EMBO Rep.* 4: 1138–1143.
42. Maeda, K., S. A. Almofty, S. K. Singh, M. M. Eid, M. Shimoda, T. Ikeda, A. Koito, P. Pham, M. F. Goodman, and N. Sakaguchi. 2013. GANP interacts with APOBEC3G and facilitates its encapsidation into the virions to reduce HIV-1 infectivity. *J. Immunol.* 191: 6030–6039.
43. Reynaud, C. A., V. Anquez, H. Grimal, and J. C. Weill. 1987. A hyperconversion mechanism generates the chicken light chain preimmune repertoire. *Cell* 48: 379–388.
44. Paddock, M. N., B. D. Buelow, S. Takeda, and A. M. Scharenberg. 2010. The BRCT domain of PARP-1 is required for immunoglobulin gene conversion. *PLoS Biol.* 8: e1000428.
45. Nakahara, M., E. Sonoda, K. Nojima, J. E. Sale, K. Takenaka, K. Kikuchi, Y. Taniguchi, K. Nakamura, Y. Sumitomo, R. T. Bree, et al. 2009. Genetic evidence for single-strand lesions initiating Nbs1-dependent homologous recombination in diversification of Ig v in chicken B lymphocytes. *PLoS Genet.* 5: e1000356.
46. Kawamoto, T., K. Araki, E. Sonoda, Y. M. Yamashita, K. Harada, K. Kikuchi, C. Masutani, F. Hanaoka, K. Nozaki, N. Hashimoto, and S. Takeda. 2005. Dual roles for DNA polymerase eta in homologous DNA recombination and translesion DNA synthesis. *Mol. Cell* 20: 793–799.
47. Campo, V. A., A. M. Patenaude, S. Kaden, L. Horb, D. Firka, J. Jiricny, and J. M. Di Noia. 2013. MSH6- or PMS2-deficiency causes re-replication in DT40 B cells, but it has little effect on immunoglobulin gene conversion or on repair of AID-generated uracils. *Nucleic Acids Res.* 41: 3032–3046.
48. Sakaguchi, N., T. Kimura, S. Matsushita, S. Fujimura, J. Shibata, M. Araki, T. Sakamoto, C. Minoda, and K. Kuwahara. 2005. Generation of high-affinity antibody against T cell-dependent antigen in the *Ganp* gene-transgenic mouse. *J. Immunol.* 174: 4485–4494.
49. Katsube, T., M. Mori, H. Tsuji, T. Shiomi, N. Shiomi, and M. Onoda. 2011. Differences in sensitivity to DNA-damaging agents between XRCC4- and Artemis-deficient human cells. *J. Radiat. Res. (Tokyo)* 52: 415–424.
50. Shibata, A., S. Conrad, J. Birraux, V. Geuting, O. Barton, A. Ismail, A. Kakarougkas, K. Meek, G. Taucher-Scholz, M. Löbrich, and P. A. Jeggo. 2011. Factors determining DNA double-strand break repair pathway choice in G_2 phase. *EMBO J.* 30: 1079–1092.
51. Abe, T., M. Ishiai, Y. Hosono, A. Yoshimura, S. Tada, N. Adachi, H. Koyama, M. Takata, S. Takeda, T. Enomoto, and M. Seki. 2008. KU70/80, DNA-PKcs, and Artemis are essential for the rapid induction of apoptosis after massive DSB formation. *Cell. Signal.* 20: 1978–1985.
52. Adachi, N., S. So, and H. Koyama. 2004. Loss of nonhomologous end joining confers camptothecin resistance in DT40 cells. Implications for the repair of topoisomerase I-mediated DNA damage. *J. Biol. Chem.* 279: 37343–37348.
53. Cook, A. J., J. M. Raftery, K. K. Lau, A. Jessup, R. S. Harris, S. Takeda, and C. J. Jolly. 2007. DNA-dependent protein kinase inhibits AID-induced antibody gene conversion. *PLoS Biol.* 5: e80.
54. Neal, J. A., V. Dang, P. Douglas, M. S. Wold, S. P. Lees-Miller, and K. Meek. 2011. Inhibition of homologous recombination by DNA-dependent protein kinase requires kinase activity, is titratable, and is modulated by autophosphorylation. *Mol. Cell. Biol.* 31: 1719–1733.
55. Convery, E., E. K. Shin, Q. Ding, W. Wang, P. Douglas, L. S. Davis, J. A. Nickoloff, S. P. Lees-Miller, and K. Meek. 2005. Inhibition of homologous recombination by variants of the catalytic subunit of the DNA-dependent protein kinase (DNA-PKcs). *Proc. Natl. Acad. Sci. USA* 102: 1345–1350.
56. Allen, C., A. Kurimasa, M. A. Brenneman, D. J. Chen, and J. A. Nickoloff. 2002. DNA-dependent protein kinase suppresses double-strand break-induced and spontaneous homologous recombination. *Proc. Natl. Acad. Sci. USA* 99: 3758–3763.
57. Wang, M., W. Wu, W. Wu, B. Rosidi, L. Zhang, H. Wang, and G. Iliakis. 2006. PARP-1 and Ku compete for repair of DNA double strand breaks by distinct NHEJ pathways. *Nucleic Acids Res.* 34: 6170–6182.
58. Adachi, N., T. Ishino, Y. Ishii, S. Takeda, and H. Koyama. 2001. DNA ligase IV-deficient cells are more resistant to ionizing radiation in the absence of Ku70: implications for DNA double-strand break repair. *Proc. Natl. Acad. Sci. USA* 98: 12109–12113.
59. Wu, X., P. Geraldes, J. L. Platt, and M. Cascalho. 2005. The double-edged sword of activation-induced cytidine deaminase. *J. Immunol.* 174: 934–941.
60. Frieder, D., M. Larijani, E. Tang, J. Y. Parsa, W. Basit, and A. Martin. 2006. Antibody diversification: mutational mechanisms and oncogenesis. *Immunol. Res.* 35: 75–88.
61. Willmore, E., S. de Caux, N. J. Sunter, M. J. Tilby, G. H. Jackson, C. A. Austin, and B. W. Durkacz. 2004. A novel DNA-dependent protein kinase inhibitor, NU7026, potentiates the cytotoxicity of topoisomerase II poisons used in the treatment of leukemia. *Blood* 103: 4659–4665.
62. Ding, Q., Y. V. Reddy, W. Wang, T. Woods, P. Douglas, D. A. Ramsden, S. P. Lees-Miller, and K. Meek. 2003. Autophosphorylation of the catalytic subunit of the DNA-dependent protein kinase is required for efficient end processing during DNA double-strand break repair. *Mol. Cell. Biol.* 23: 5836–5848.
63. Li, Z., C. J. Woo, M. D. Iglesias-Ussel, D. Ronai, and M. D. Scharff. 2004. The generation of antibody diversity through somatic hypermutation and class switch recombination. *Genes Dev.* 18: 1–11.
64. Barreto, V., B. Reina-San-Martin, A. R. Ramiro, K. M. McBride, and M. C. Nussenzweig. 2003. C-terminal deletion of AID uncouples class switch recombination from somatic hypermutation and gene conversion. *Mol. Cell* 12: 501–508.
65. Liu, M., J. L. Duke, D. J. Richter, C. G. Vinuesa, C. C. Goodnow, S. H. Kleinstein, and D. G. Schatz. 2008. Two levels of protection for the B cell genome during somatic hypermutation. *Nature* 451: 841–845.
66. Mierau, M., G. A. Drexler, A. Kutzera, K. Braunschmidt, J. Ellwart, F. Eckardt-Schupp, E. Fritz, J. Bachl, and B. Jungnickel. 2008. Non-conservative homologous recombination in human B lymphocytes is promoted by activation-induced cytidine deaminase and transcription. *Nucleic Acids Res.* 36: 5591–5601.
67. Li, Z., C. Zhao, M. D. Iglesias-Ussel, Z. Polonskaya, M. Zhuang, G. Yang, Z. Luo, W. Edelmann, and M. D. Scharff. 2006. The mismatch repair protein Msh6 influences the in vivo AID targeting to the Ig locus. *Immunity* 24: 393–403.
68. Allen, C., J. Halbrook, and J. A. Nickoloff. 2003. Interactive competition between homologous recombination and non-homologous end joining. *Mol. Cancer Res.* 1: 913–920.
69. Küppers, R., and R. Dalla-Favera. 2001. Mechanisms of chromosomal translocations in B cell lymphomas. *Oncogene* 20: 5580–5594.
70. Goossens, T., U. Klein, and R. Küppers. 1998. Frequent occurrence of deletions and duplications during somatic hypermutation: implications for oncogene translocations and heavy chain disease. *Proc. Natl. Acad. Sci. USA* 95: 2463–2468.
71. Bemark, M., J. E. Sale, H. J. Kim, C. Berek, R. A. Cosgrove, and M. S. Neuberger. 2000. Somatic hypermutation in the absence of DNA-dependent protein kinase catalytic subunit (DNA-PK(cs)) or recombination-activating gene (RAG)1 activity. *J. Exp. Med.* 192: 1509–1514.
72. Cook, A. J., L. Oganesian, P. Harumal, A. Basten, R. Brink, and C. J. Jolly. 2003. Reduced switching in SCID B cells is associated with altered somatic mutation of recombined S regions. *J. Immunol.* 171: 6556–6564.